Realistic Investigations of Materials with Strong Electronic Correlations

Dieter Vollhardt

Supported by Deutsche Forschungsgemeinschaft through SFB 484

1. Introduction:

- DFT/LDA vs. model approaches
- Dynamical mean-field theory (DMFT)
- Single-impurity physics
- LDA + DMFT

2. Applications:

- $(La, Sr)\,TiO_3$
- V_2O_3
- $(Ca, Sr)\,VO_3$

[- LiV_2O_4]

- How much LDA-input is necessary?

3. Questions

Photoemission on $La_{1-x}Sr_xTiO_3$, $x = 0.06$

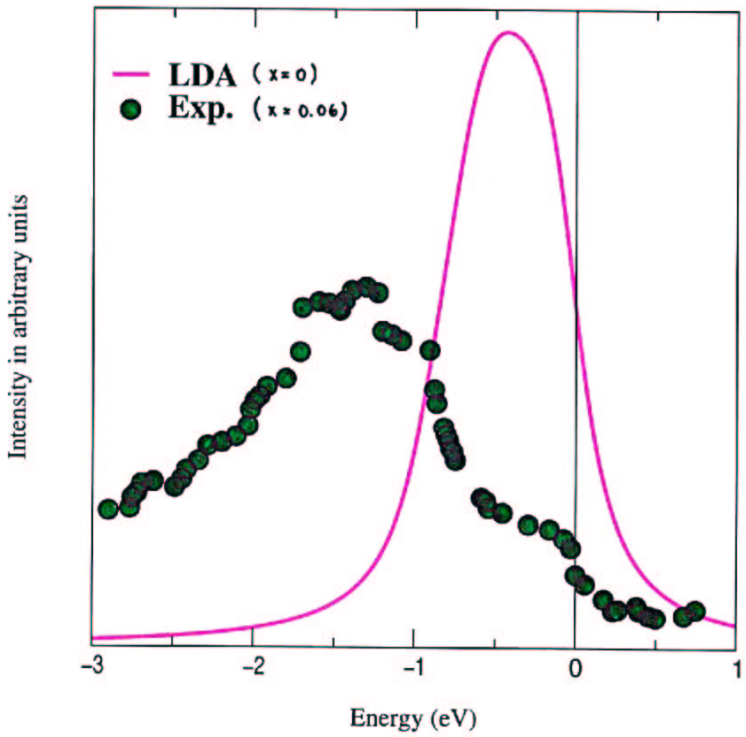

Comparison of the experimental photoemission spectrum [Fujimori et al., PRL **69**, 1796 (1992)] to the LDA result.

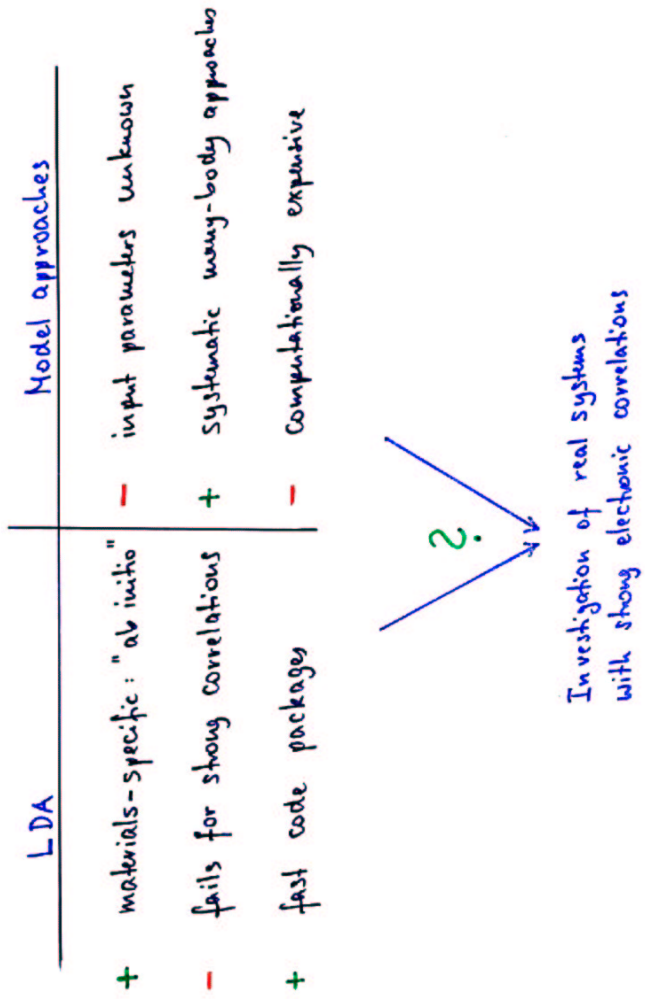

How to include correlations ?

LDA + U — Anisimov, Zaanen, Andersen (1991)

But: genuine correlation effect are due to many-body dynamics: $\Sigma(\omega)$

LDA + U^2 — Steiner, Albers, Sham (1992)

⋮

LDA + DMFT — Anisimov, Poteryaev, Korotin, Anokhin, Kotliar (1997)

LDA^{++} — Lichtenstein, Katsnelson (1998)

GW + DMFT — Biermann, Aryasetiawan, Georges ('02)

⋮

DFT + multi-band Gutzwiller WF — Bünemann, Gebhard, Weber ('98)

Models Approach

$$H = \sum_{ij,\sigma} t_{ij} c^{\dagger}_{i\sigma} c_{j\sigma} + U \sum_i n_{i\uparrow} n_{i\downarrow}$$

$n=1$:

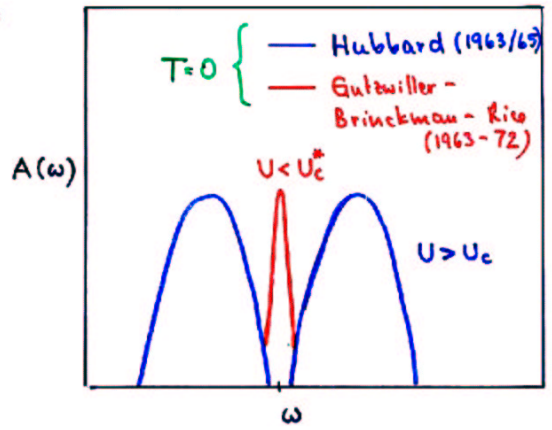

Coherent, thermodynamically consistent framework ?

From the $d \to \infty$ limit to dynamical mean-field theory (DMFT)

Metzner, Vollhardt (1989)

Real lattice system

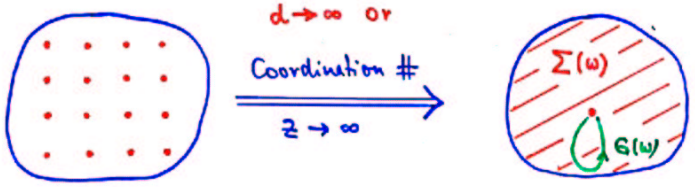

Self-energy $\Sigma_{ij}(\omega) \longrightarrow \Sigma(\omega)\,\delta_{ij}$

Propagator $G_{ij}(\omega) \longrightarrow G(\omega)\,\delta_{ij}$

- Dynamics fully included
- Spatial dependence simplified

Müller-Hartmann (1989)

1) $$G(\omega) = \int d\varepsilon \, \frac{N^0(\varepsilon)}{\omega + \mu - \varepsilon - \Sigma(\omega)} = G^0(\omega - \Sigma(\omega))$$

2) $$G(\omega) = -\frac{1}{Z} \int \mathcal{D}[\psi,\psi^*]\, \psi\, \psi^*\, e^{\mathcal{A}}$$

Brandt, Mielsch (1989)
Janis (1991)

single-site action: $\mathcal{A} \sim \underbrace{\text{kinetic energy}}_{\mathcal{G}^{-1}} - \underbrace{\text{potential energy}}_{U n_\uparrow n_\downarrow - \Sigma}$

$$= \text{tr}\, \psi^* [\underbrace{\mathcal{G}^{-1} + \Sigma}_{\mathcal{G}_0^{-1}}] \psi - U \int_0^\beta d\tau\, n_\uparrow(\tau) n_\downarrow(\tau)$$

$\hat{=}$ Single-impurity ("Anderson") problem

Georges, Kotliar (1992)

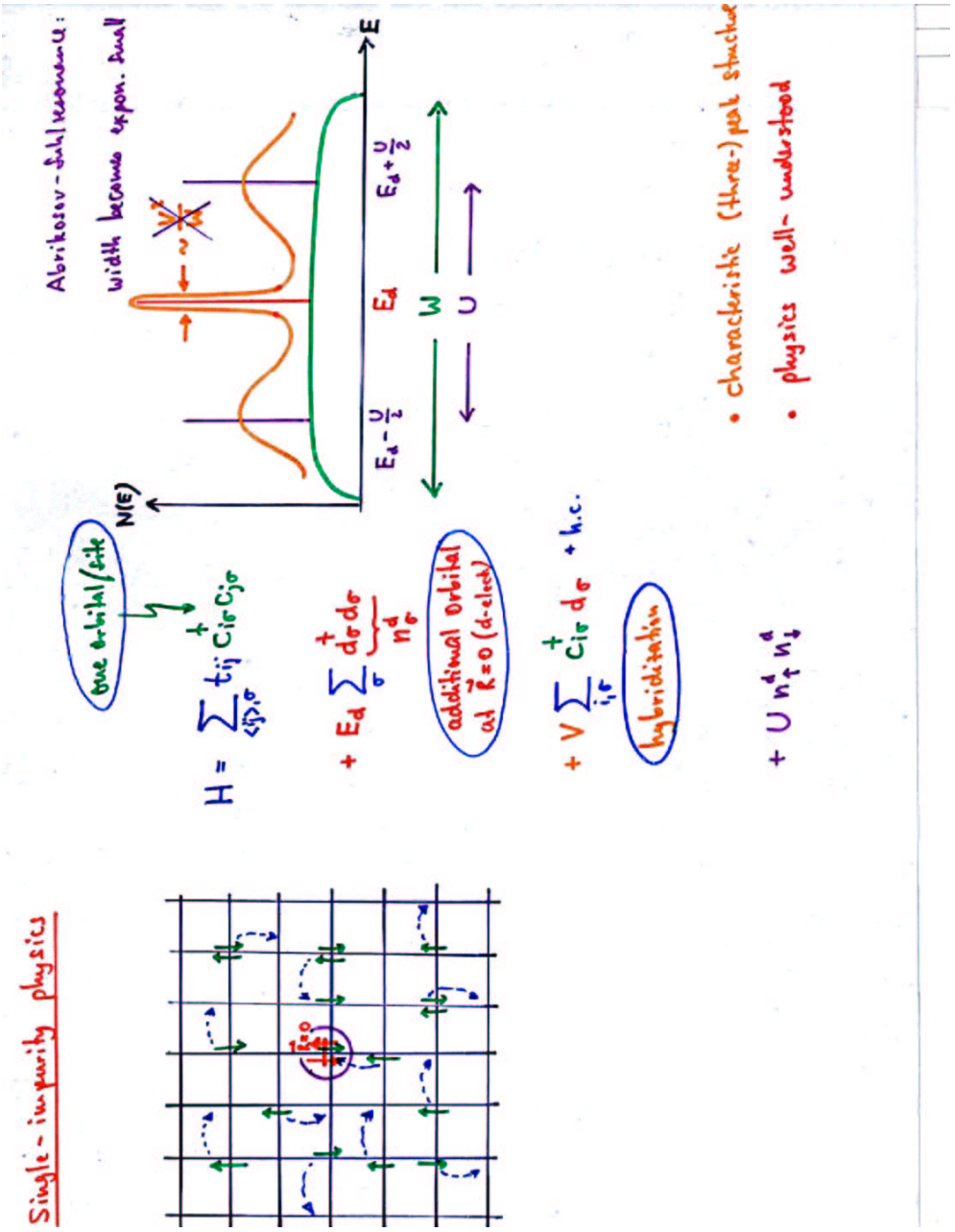

Single-impurity physics

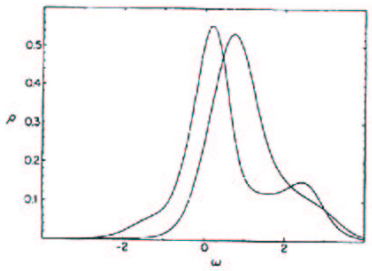

FIG. 1. Local spectral density for $U=2.5$ and densities $n=0.6$, $n=0.2$ (from left to right), obtained by the procedure described in the text.

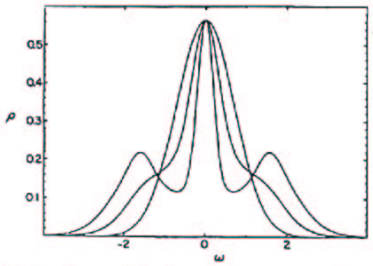

FIG. 2. Local spectral density of the paramagnetic solution at half filling ($n=1$) for $U=0$, $U=1.5$, and $U=2.5$.

cal moment regime for large U is likely to arise only quite close to $n=1$ for large U. Most densities are then in the mixed-valence regime, with the dilute regime setting in roughly near the Hartree-Fock boundary.

Finally, we present results obtained by solving (3)–(5) using second-order perturbation theory for the single-site dynamics (3). A previous weak-coupling study was carried out by Müller-Hartmann,[10] using self-consistent perturbation theory, i.e., inserting the full propagator G into the calculation of the second-order proper irreducible self-energy. Our method and results differ significantly from this approach. Indeed, it has been shown by Yosida and Yamada[11] that perturbation theory in U is quite well behaved for the Anderson model, *provided the expansion is made around the nonmagnetic Hartree-Fock solution,* i.e., that $U(n_\uparrow - n/2)(n_\downarrow - n/2)$ is treated as a perturbation. Only this procedure is able to handle correctly the

approaches, in contrast to direct perturbation theory. The Hartree shift is responsible for the appearance of the upper-band satellite peaks, as also pointed out recently by Schweitzer and Czycholl at half-filling in a related context [Ref. 14 has results qualitatively close to ours; the effect of satisfying (5) is to push down the upper band to lower energies and to somewhat reduce Z further].

As a conclusion, we believe that the infinite-dimensional Hubbard model provides a very natural mean-field description of strongly correlated Fermi liquids. It captures both the itinerant and atomic aspects and their interplay, which is at the heart of the strong correlation problem. The connection to a single-impurity problem clarifies the analytic structure of the perturbation theory in the weak- and strong-coupling regimes, it explains how the Hubbard bands emerge in the spectral function of the Hubbard model, and suggests useful approximation schemes to extract the essential physics of the Hubbard

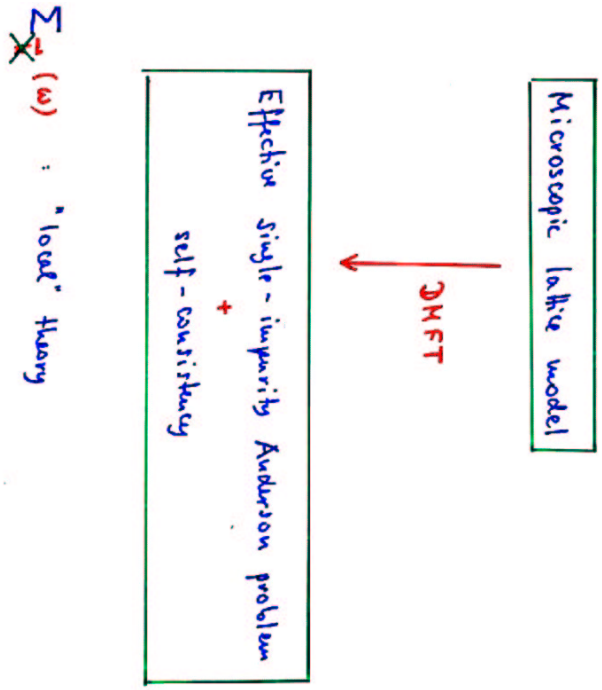

Dr. Dieter Vollhardt, Univ Augsburg (KITP 7-31-02) Realistic Investigations of Materials with Strong Electronic Correlations

Set-up for LDA + many-body theory

Anisimov et al. (1997)
Lichtenstein, Katsnelson (1998)

$$\hat{H} = \underbrace{\hat{H}^{LDA}\{t_{ilm,jl'm'}, \varepsilon_{ilm}\}}_{\text{LDA-LMTO}} + \underbrace{\hat{H}_{corr}\{U^{\sigma\sigma'}_{mm'}, J_{mm'}\}}_{\text{local correl.}} - \underbrace{\hat{H}^{LDA}_{U}}_{\text{Coulomb Correl. in } \hat{H}^{LDA}}$$

$\downarrow$ E^{LDA} (total LDA energy)

$\downarrow$ E^{LDA}_{U} (average Correl. energy in LDA)

$$\varepsilon^{0}_{ilm} := \frac{d}{dn_{ilm}}\left(E^{LDA} - E^{LDA}_{U}\right)$$

$\Rightarrow$ "ab initio Hamiltonian"

$$\hat{H}_{LDA+corr} = \underbrace{\hat{H}^{LDA}\{t_{ilm,jl'm'}, \varepsilon^{0}_{ilm}\}}_{\hat{H}^{LDA}_{0}} + \hat{H}_{corr}\{U^{\sigma\sigma'}_{mm'}, J_{mm'}\}$$

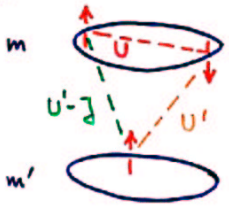

G. Keller et al. (2002)

Comparison between LDA and LDA+DMFT(QMC) at $U = 0$; V_2O_3

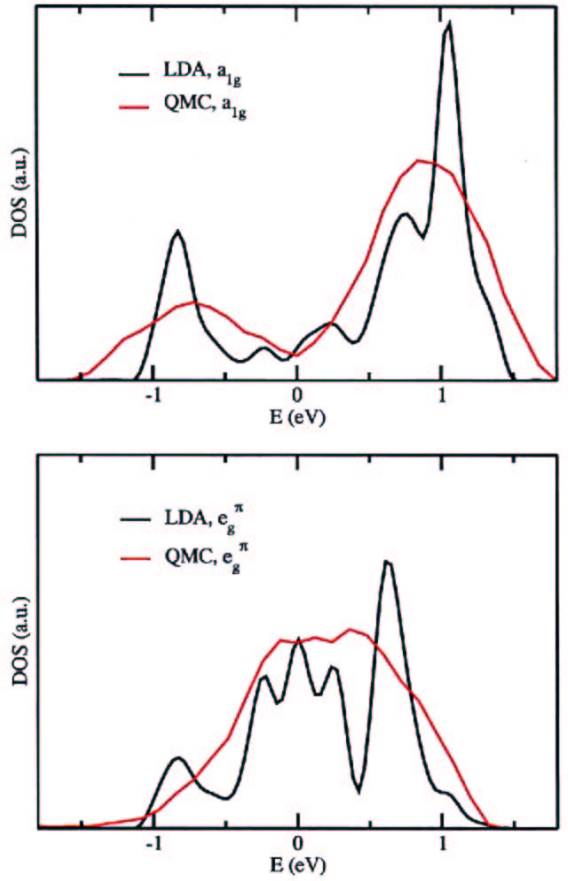

QMC-Simulations at $T = 1100$ K and $U = 0$ eV

Comparison between LDA and LDA+DMFT(QMC) at $U = 0$ (with broadening)

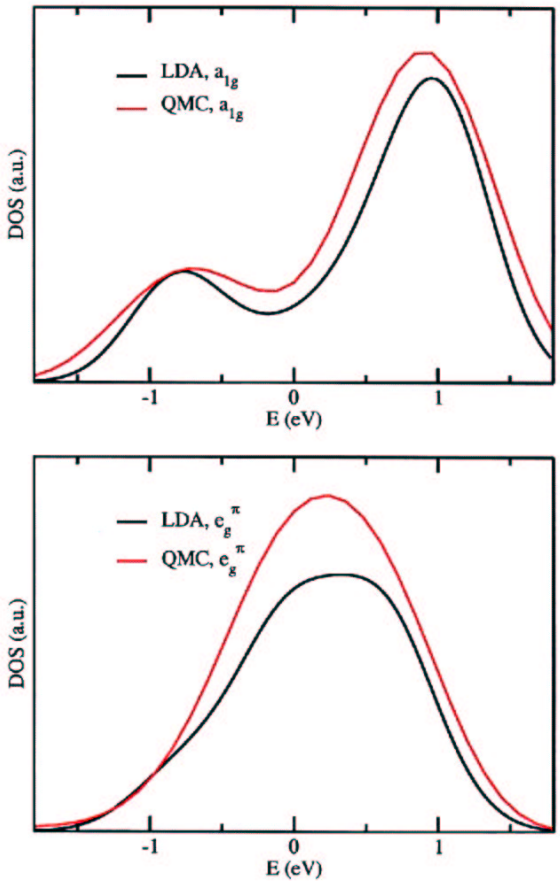

QMC-Simulations at $T = 1100$ K and $U = 0$ eV, assumed broadening for LDA and LDA+DMFT 0.3 eV

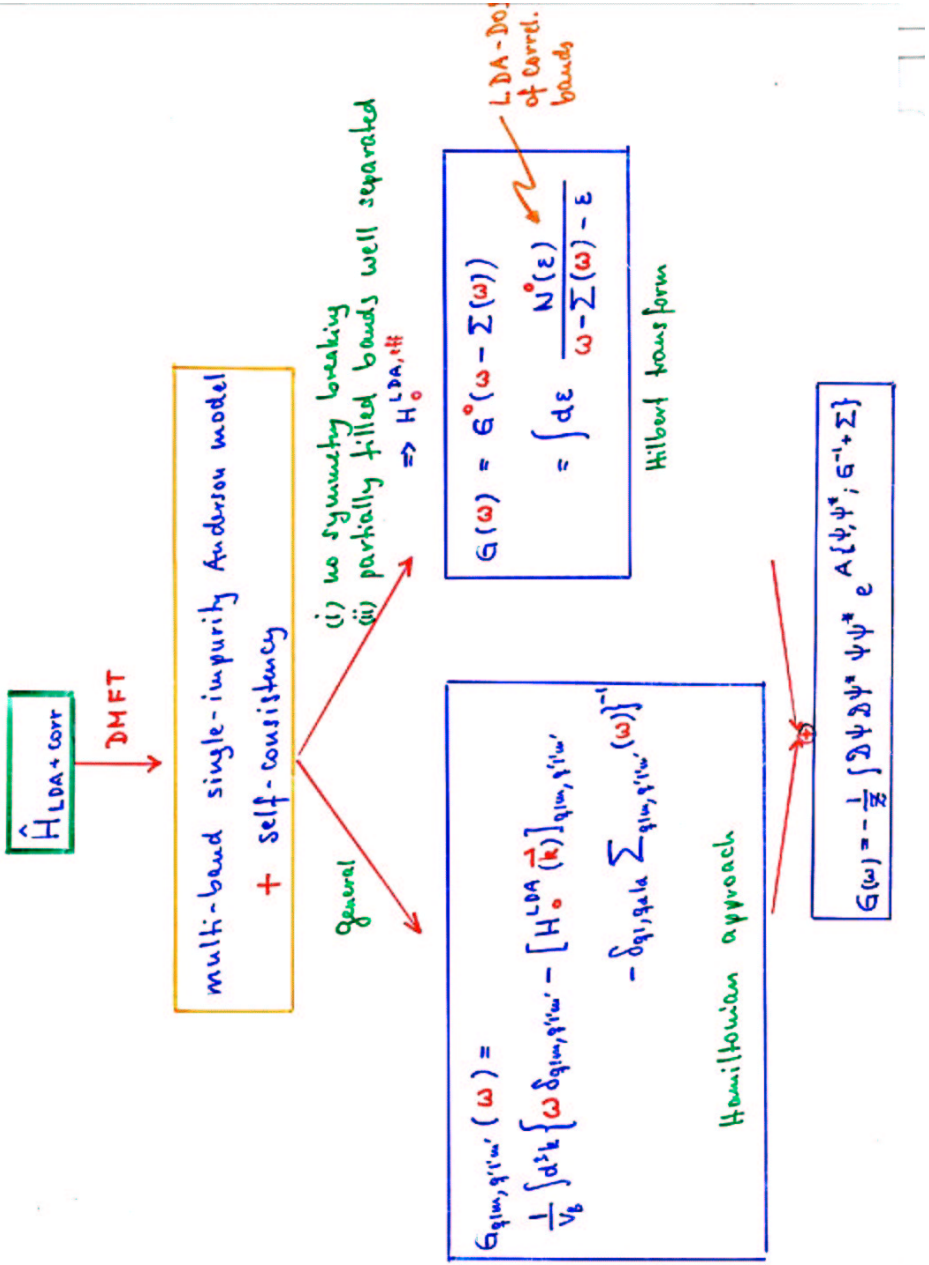

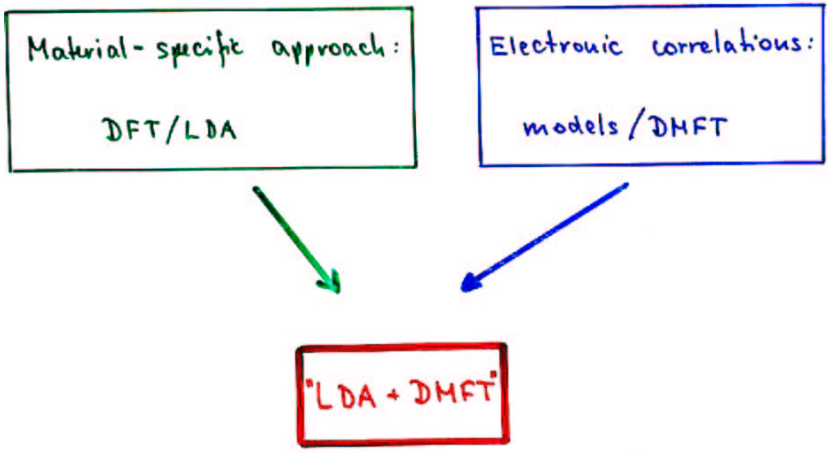

Dynamical mean-field theory (DMFT) for $\hat{H}_{LDA+corr}$

⇓

LDA + DMFT (X)

X: single-impurity solver IPT, NCA, QMC

Alternatives ?

- NRG
- Flow equ. approach

Application to $La_{1-x}Sr_xTiO_3$

$LaTiO_3$

Cubic perowskite

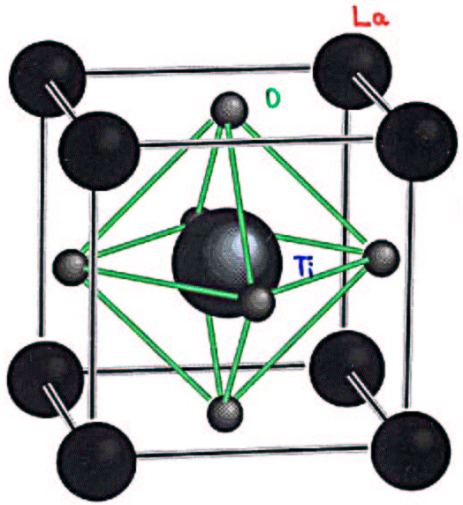

$T < T_N \approx 125\,K$: AF insulator

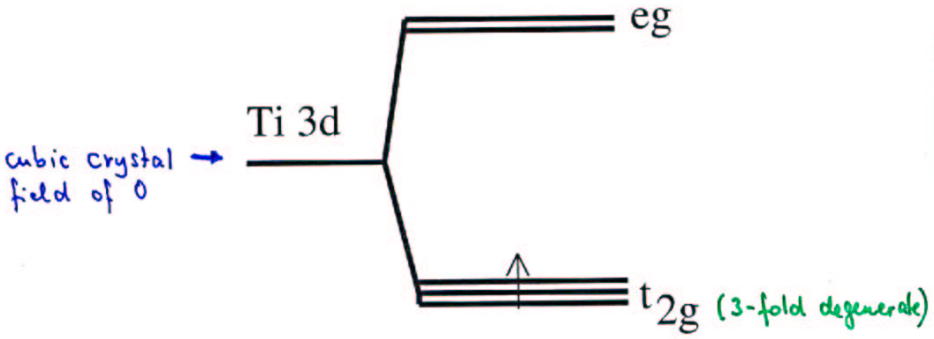

Sr - doping $x \gtrsim 5\%$: strongly correlated paramagnetic metal

$LaTiO_3$: partial t_{2g} density of states

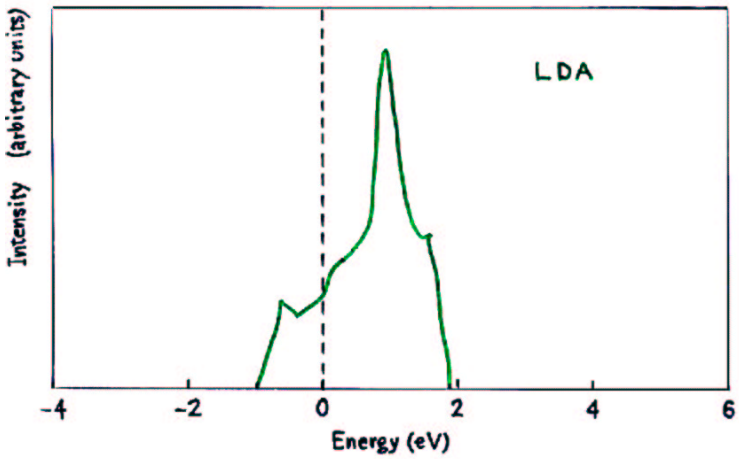

Input to DMFT

$x=6\%: La_{1-x}Sr_xTiO_3$: $U^{LDA} = 4.2 \pm 1$ eV

Sensitive dependence on orthogon. of WF + choice of orbitals : TB-LMTO-ASA
ASA-LMTO
⋮

Need "best possible" LDA values for U, J, ...

$La_{1-x}Sr_xTiO_3$: Results from LDA+DMFT(QMC)

Nekrasov, Held, Blümer, Poteryaev, Anisimov, Vollhardt
Eur. Phys. J. B **18**, 55 (2000)

Partial t_{2g} densities of states

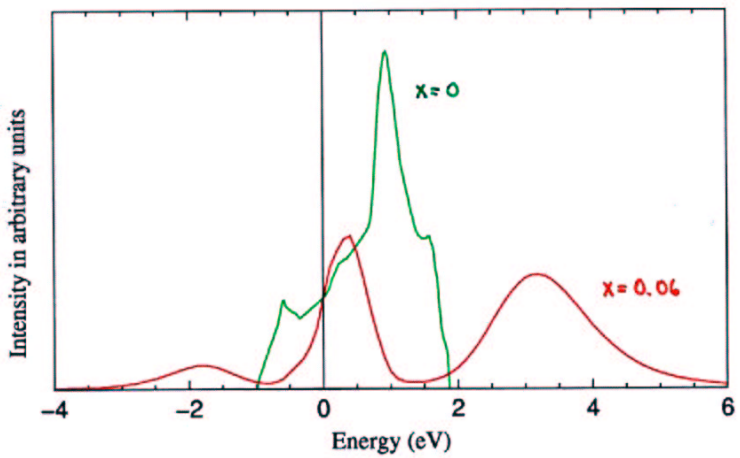

LDA (—) LDA+DMFT(QMC) (—)

Parameters for DMFT:
$x = 0.06$, $U = 4.0$ eV, $T = 0.1$ eV$\sim$ 1000K, 3 degenerate bands

Comparison with experiment

Nekrasov, Held, Blümer, Poteryaev, Anisimov, Vollhardt
Eur. Phys. J. B **18**, 55 (2000)

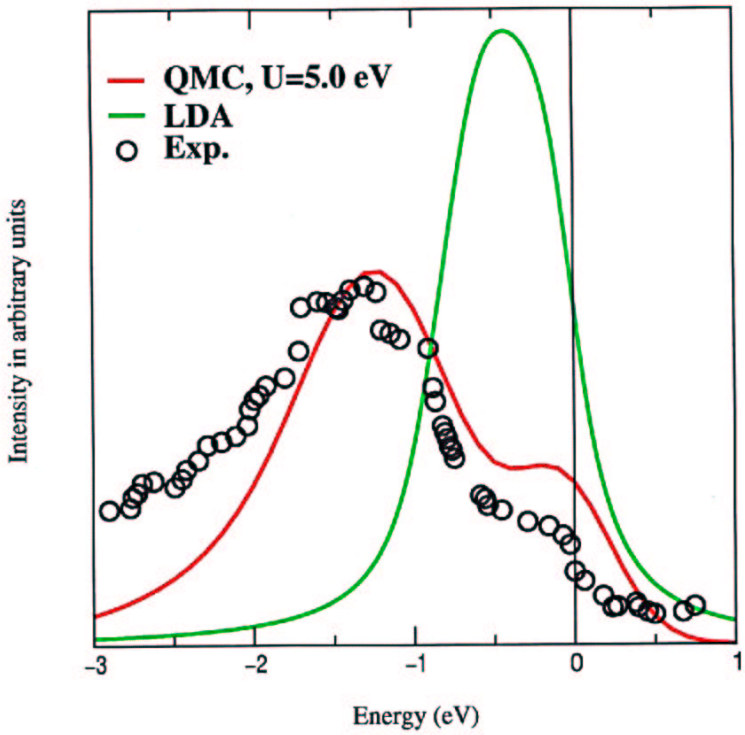

Comparison of the experimental photoemission spectrum ($T = 80$ K, resolution $\Delta\varepsilon = 0.3$ eV) [Fujimori et al., PRL **69**, 1796 (1992)], the LDA result ($T = 0$), and the LDA+DMFT(QMC) calculation ($T = 1000$ K) for $LaTiO_3$ with 6% hole doping.

Application to V_2O_3

Mott-Hubbard Metal-Insulator Transition in V_2O_3

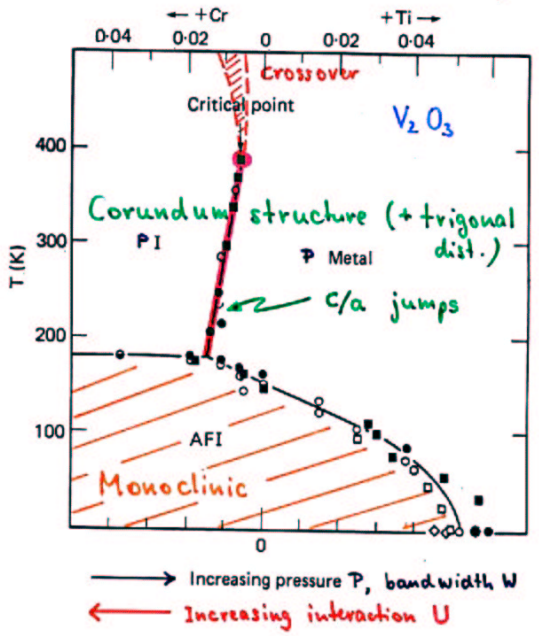

PI → PM:

1) 1. order transition, but no change in crystal symmetry

2) $\frac{dU}{dT} < 0 \Longrightarrow S_I > S_M$ ↔ „Pomeranchuk

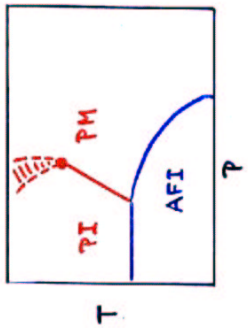

⇒ MIT driven by electronic interactions

Material-specific input

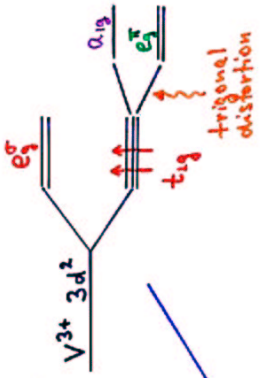

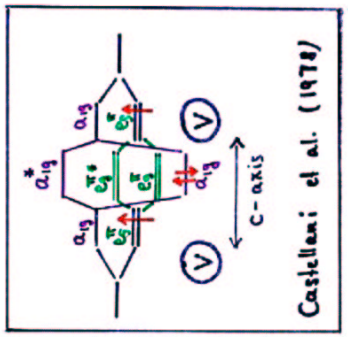

effective $S=\frac{1}{2}$ model, 2-fold degeneracy

Models approach

ne-band Hubbard model

$(S=\frac{1}{2}$, n=1, "frustrated" AF)

Spin state of V_2O_3

Crystal structure

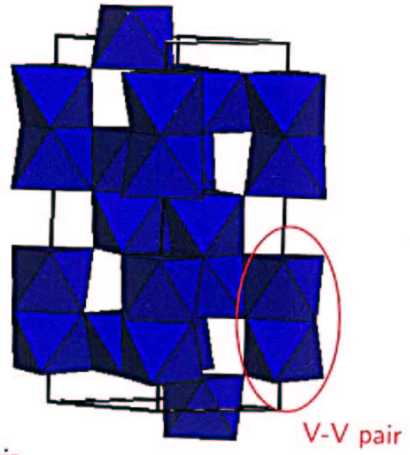

↑
c-axis

a_{1g}-splitting

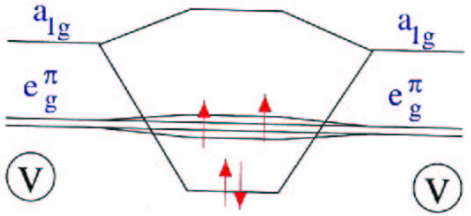

Castellani et al. '78 → Spin $S = \frac{1}{2}$

Caskellani et al. (1978) : 1 spin / V in e_g^π orbital
⇒ $S = \frac{1}{2}$ model

But:

Park et al. (2000) : polarized x-ray spectroscopy
$S = 1$ state, $e_g^\pi e_g^\pi \oplus e_g^\pi a_{1g}$ Conf's.

Ezhov et al. (1999) LDA + U
Mila et al. (2000)
AFI
$e_g^\pi e_g^\pi$, no orbital degeneracy
$S = 1$ state
orbital degeneracy

→ theory for the paramagnetic phase ?

(i) LDA results for V_2O_3

Held, Keller, Eyert, Vollhardt, Anisimov (2001)

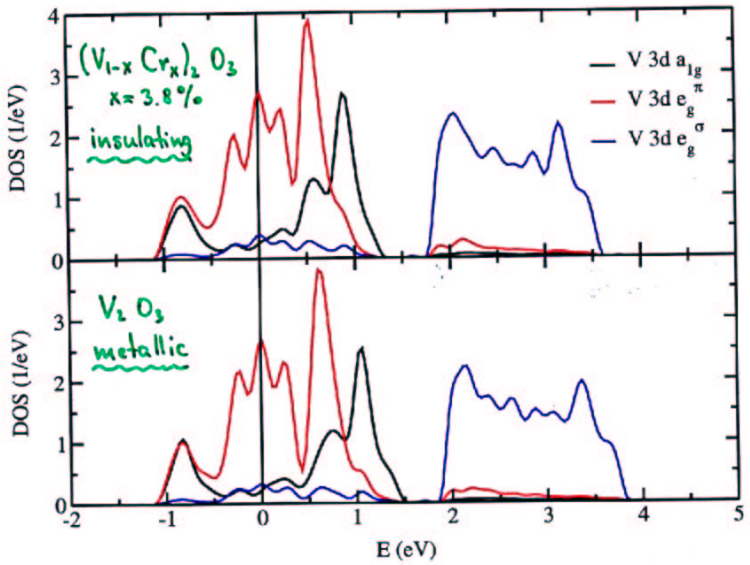

Total and partial densities of states (DOS) of V_2O_3 (metallic paramagnetic phase) and $(V_{0.962}Cr_{0.038})_2O_3$ (insulating paramagnetic phase) per unit cell

PI/PM : Corundum structure

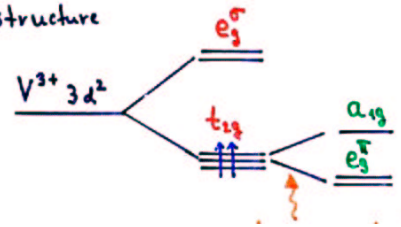

(ii) Introduce electronic correlations by LDA + DMFT (QMC)

Held, Keller, Eyert, Vollhardt, Anisimov, PRL 2001

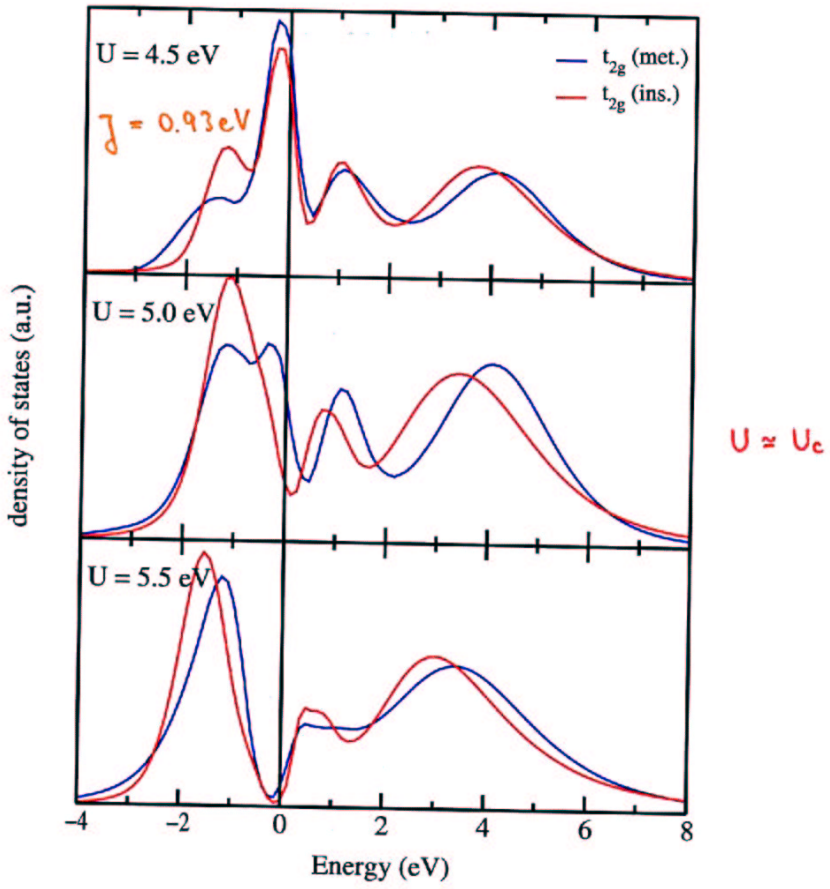

U ≃ U_c

LDA+DMFT(QMC) spectra for paramagnetic $(V_{0.962}Cr_{0.038})_2O_3$ ("ins.") and V_2O_3 ("met.") for $U = 4.5$, 5, 5.5 eV; $T = 1100$ K.

V_2O_3

Held, Keller, Eyert, Vollhardt, Anisimov [PRL **86**, 5345 (2001)]

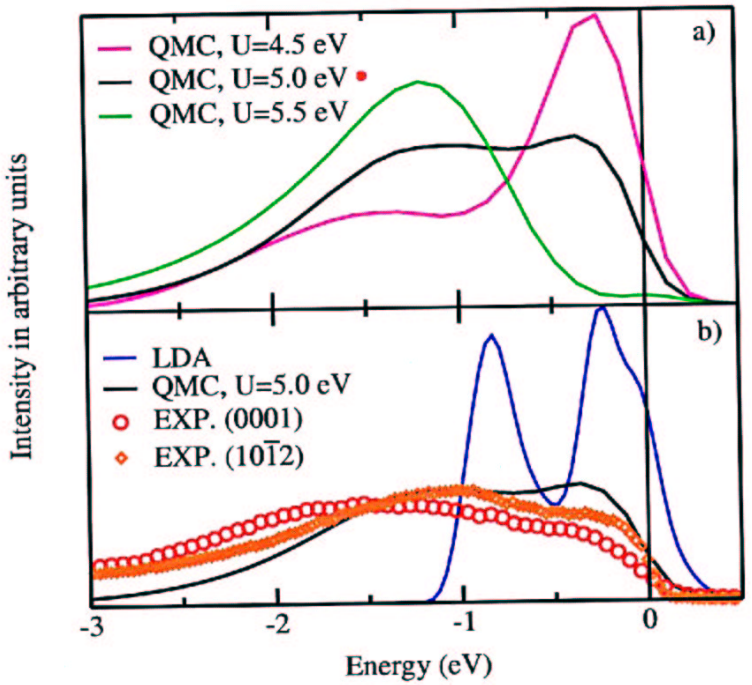

a) Comparison of LDA+DMFT(QMC) calculations for $U = 4.5$, $U = 5.0$ and $U = 5.5$ eV

b) Comparison of the experimental photoemission spectrum [Schramme et al.], the LDA result [Eyert], and the LDA+DMFT(QMC) calculation for V_2O_3 and Coulomb interaction 5.0 eV (assumed experimental resolution 0.05 eV).

Correlation parametrized by, e.g.,

$\frac{U}{W}$

- less screening at surface
- smaller coord.# ⇒ smaller band width

⇒ $\frac{U}{W}$ larger at surface

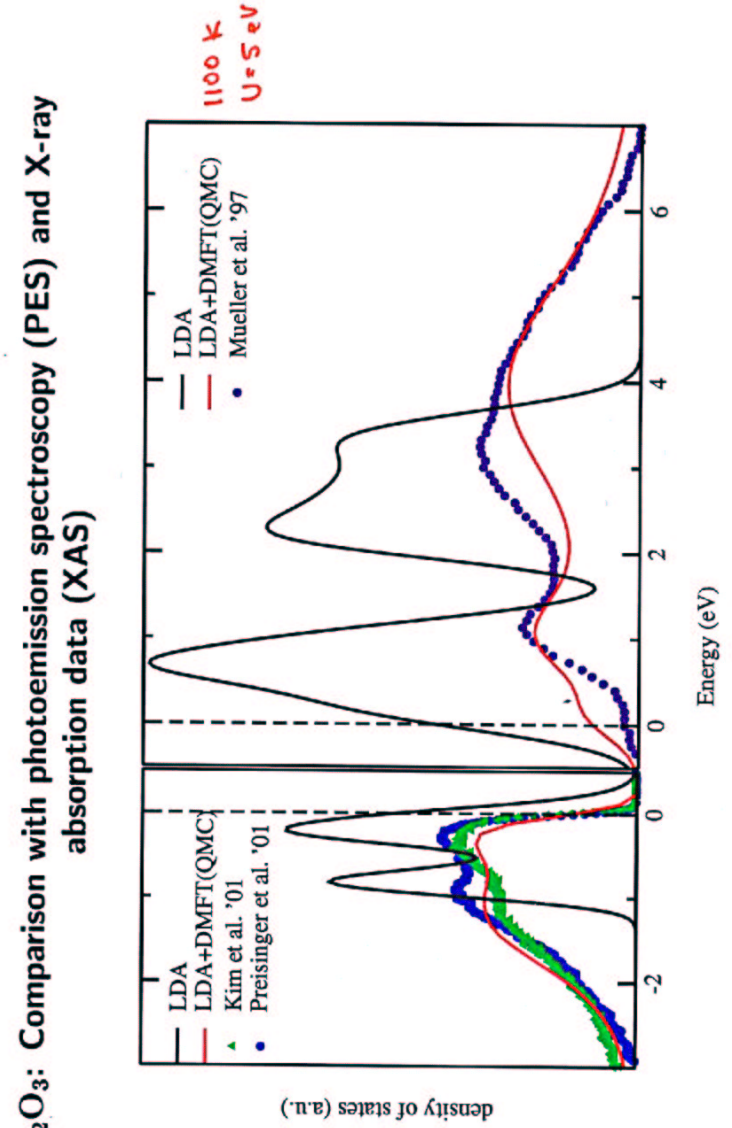

LDA+DMFT(QMC) results for metallic V_2O_3

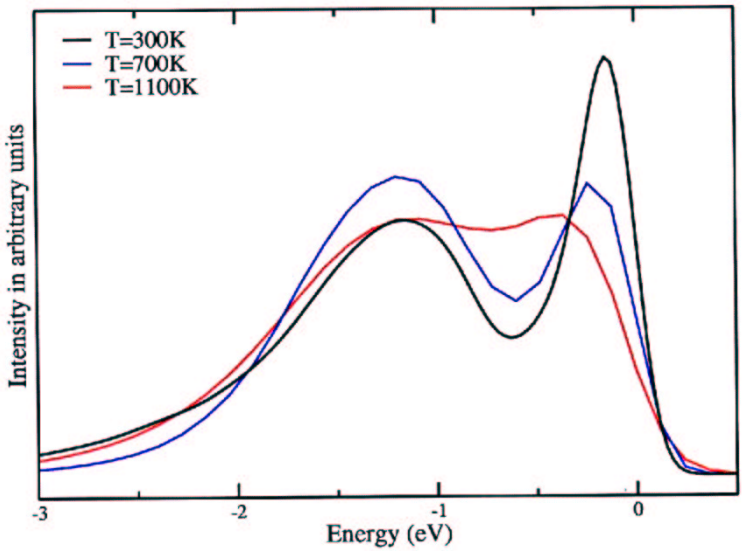

Calculations at $T = 300$ K, $T = 700$ K and $T = 1100$ K for $U = 5.0$ eV

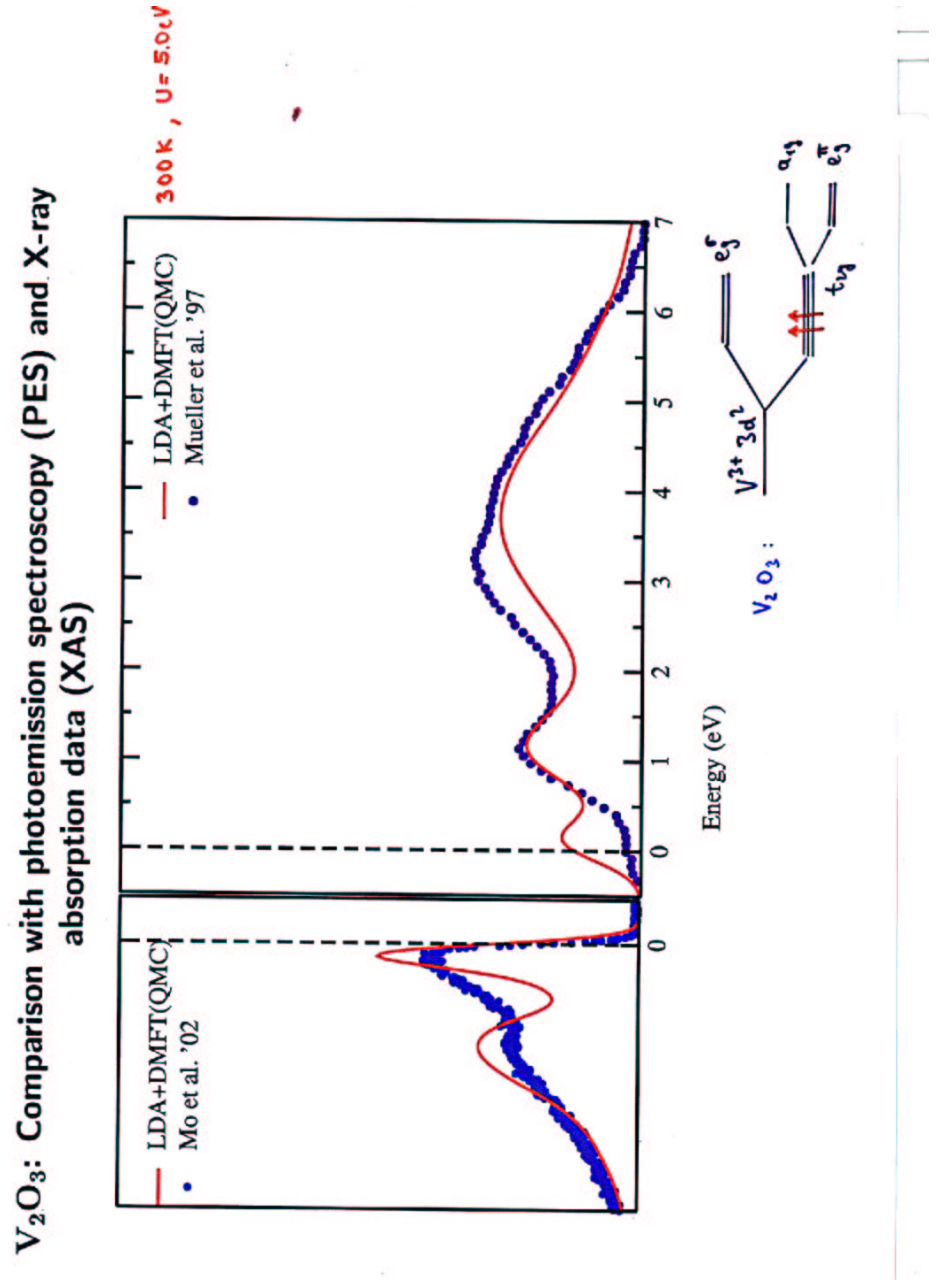

Spin state of V_2O_3

Held, Keller, Eyert, Vollhardt, Anisimov [PRL **86**, 5345 (2001)]

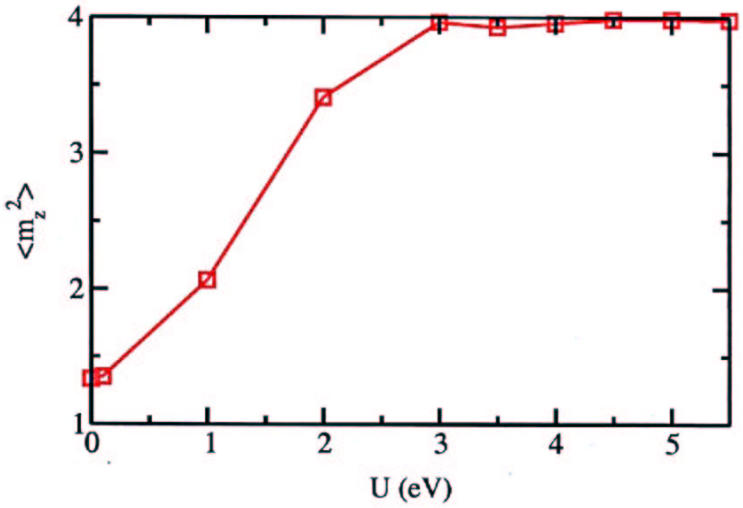

$\langle m_a^2 \rangle = \left\langle \left[\sum_{\nu=1}^{3} (\hat{n}_{\nu\uparrow} - \hat{n}_{\nu\downarrow}) \right]^2 \right\rangle \xrightarrow{U>3eV} 4$

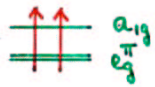

S=1 state

LDA + DMFT: How much material-specific (LDA) input is required?

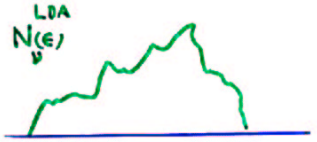

$M_\nu^{(n)} = \int d\epsilon\, \epsilon^n N_\nu^{LDA}(\epsilon)$: $\begin{cases} n=0 & \text{density} \\ n=1 & \tilde{\epsilon} \\ n=2 & (\text{bandwidth})^2 \end{cases}$

1) Degenerate bands

e.g. $LaTiO_3$

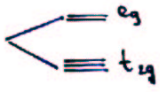

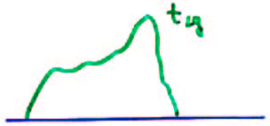

→ $M^{(2)}$

2) Non-degenerate bands

e.g. V_2O_3 (trig. splitting)

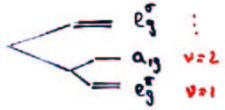

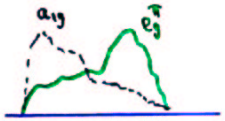

→ $M_\nu^{(1)}$, $M_\nu^{(2)}$, ($M_\nu^{(3)}$)

3) General case

- Strong hybridization of bands
- very diff. bond strengths, e.g. NaV_2O_5

→ beyond LDA DOS: Hamiltonian approach

$SrVO_3$ vs. $CaVO_3$: crystal structure

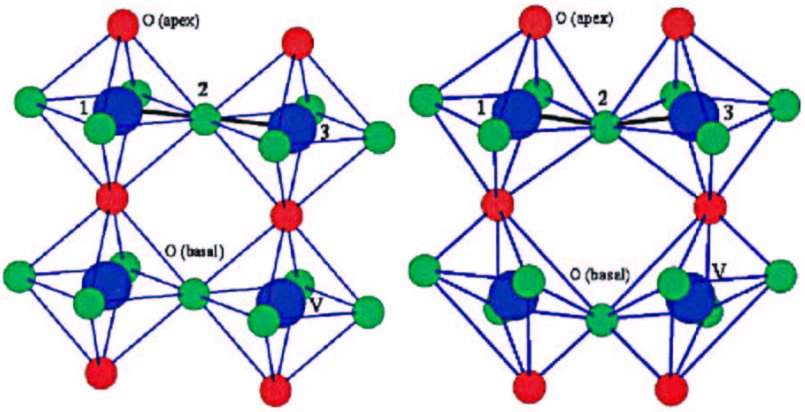

- cubic perovskite

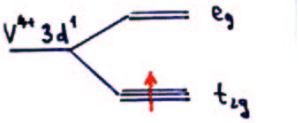

- paramagnetic metals
  thermodyn. + transport quantities of $Sr_{1-x}Ca_xVO_3$ almost indep. of x
- natural oxygen vacancies (~ 1%)

$SrVO_3$ is ideal $Fm\bar{3}m$	$CaVO_3$ is orthorhombically distorted Pbnm
$\angle 123 = 180°$	$\angle 123 = \cancel{147°}$ 160°

$\Downarrow$

main effect: reduction of $\angle 123$ $\quad |\cos\theta| = 0.94$

$\Rightarrow W_{Sr} > W_{Ca}$

1

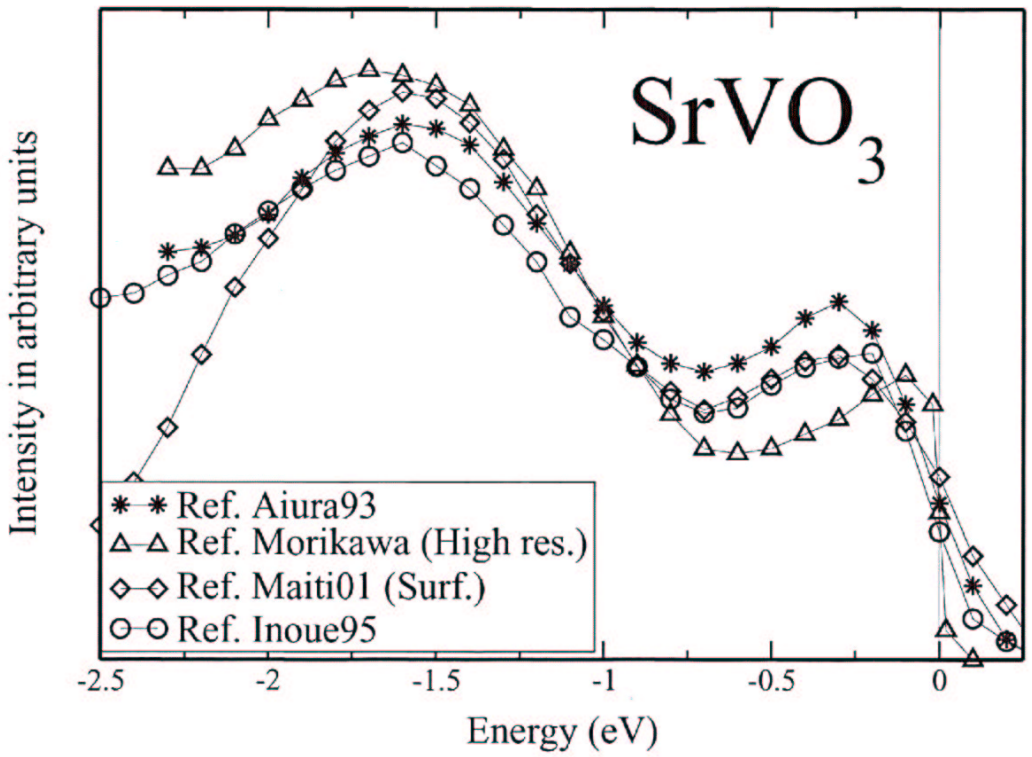

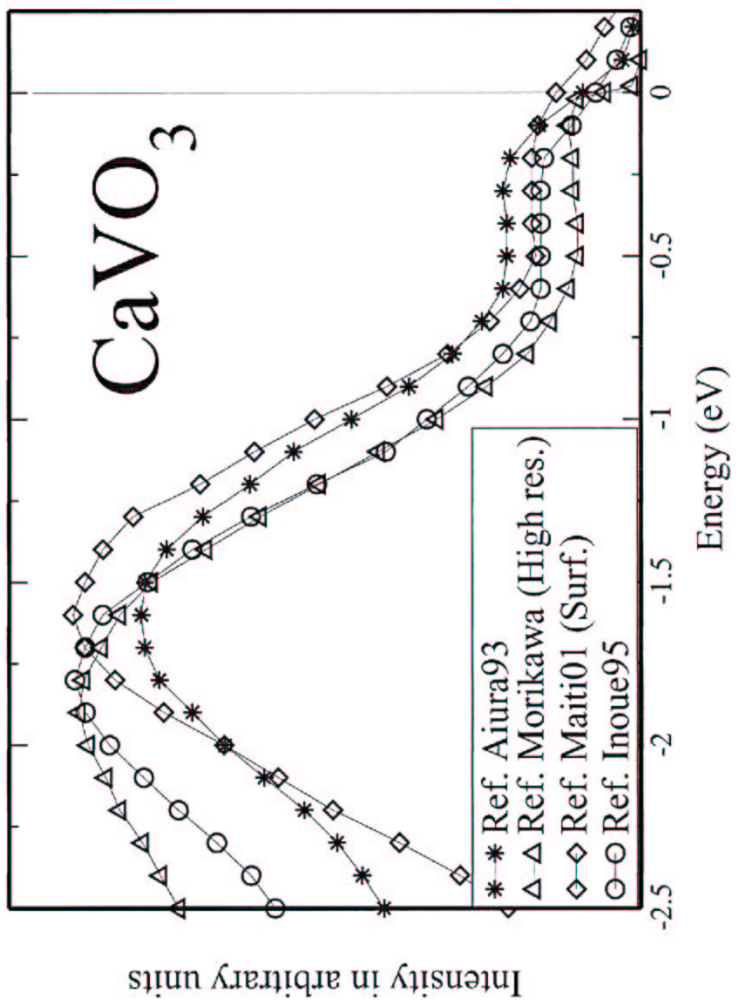
CaVO3
Ref. Aiura93
Ref. Morikawa (High res.)
Ref. Maiti01 (Surf.)
Ref. Inoue95
Intensity in arbitrary units
Energy (eV)
0
-0.5
-1
-1.5
-2
-2.5

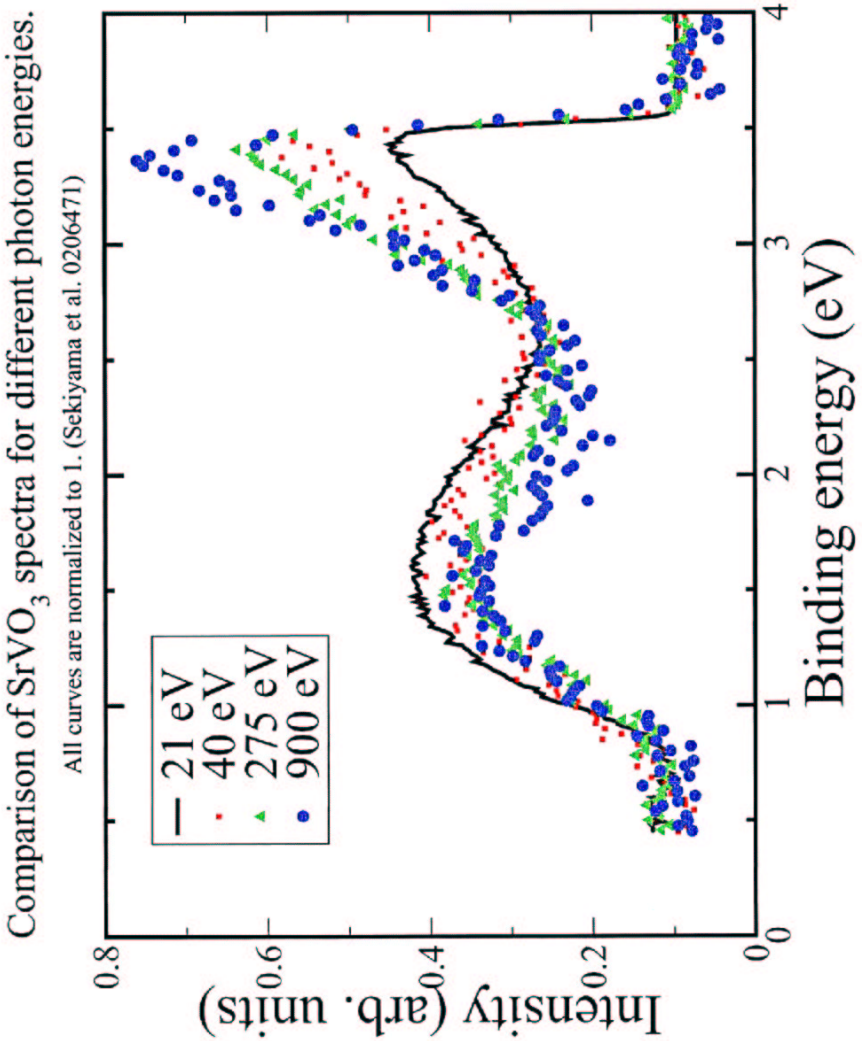
Comparison of SrVO3 spectra for different photon energies.
All curves are normalized to 1. (Sekiyama et al. 0206471)
21 eV
40 eV
275 eV
900 eV
Intensity (arb. units)
Binding energy (eV)
0
0.2
0.4
0.6
0.8
1
2
3
4

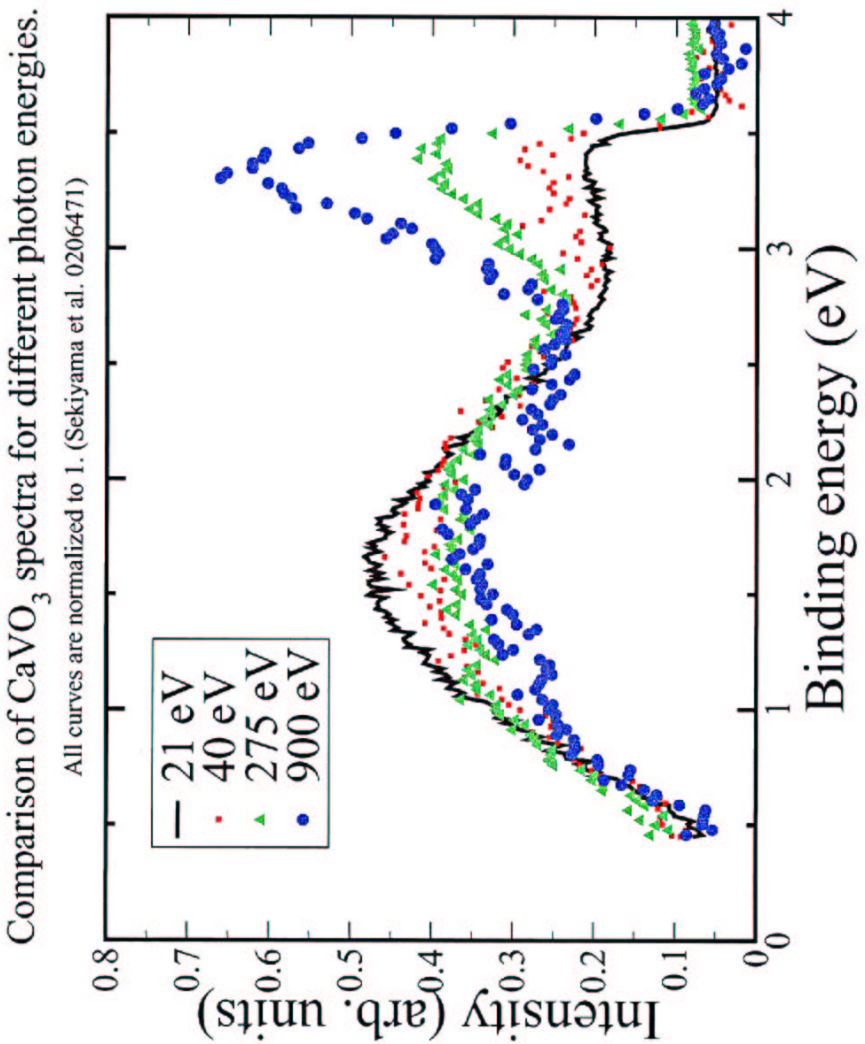
Comparison of $CaVO_3$ spectra for different photon energies.
All curves are normalized to 1. (Sekiyama et al. 0206471)
21 eV
40 eV
275 eV
900 eV
Intensity (arb. units)
Binding energy (eV)

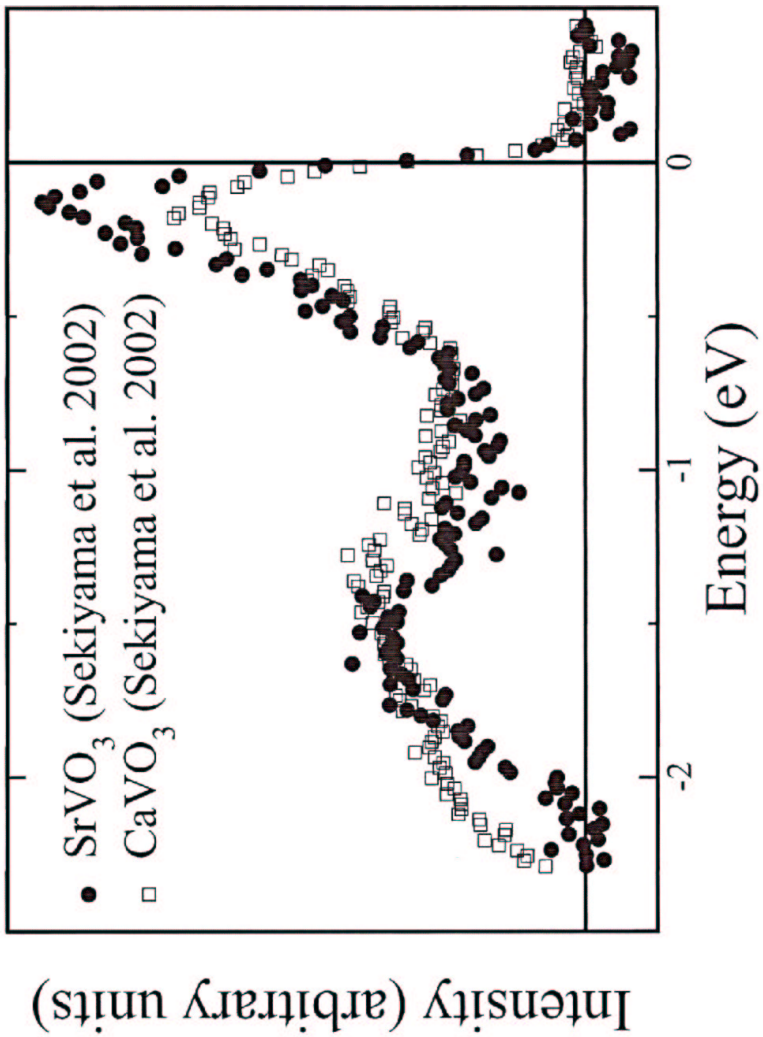
$SrVO_3$ (Sekiyama et al. 2002)
$CaVO_3$ (Sekiyama et al. 2002)
Intensity (arbitrary units)
Energy (eV)

Bulk:

$SrVO_3$ and $CaVO_3$ very similar : $|\cos\theta|$ - effect

Surface:

$CaVO_3$ considerably stronger correlated

- than in bulk
- than $SrVO_3$

vicinity of MIT ?

2

Questions:

- Can one "optimize" the LDA-calculated value of U, J,... needed as input to DMFT ?
- Is there a fast and reliable impurity solver at low T ?
- Suitable acronym for X + DMFT ? RDMF ?